Selective scandium ion capture *via* coordination templating in a covalent organic framework

Ye Yuan

Yajie Yang

Katie R. Meihaus
  University of California, Berkeley, California 94720

Shenli Zhang
  Pritzker School of Molecular Engineering, University of Chicago, Chicago, IL 60615
  https://orcid.org/0000-0001-9907-9967

Xin Ge
  Electron Microscopy Center, Jilin University

Wei Zhang
  Jilin University   https://orcid.org/0000-0002-6414-7015

Roland Faller
  Department of Chemical Engineering, University of California, Davis, CA 95616   https://orcid.org/0000-0001-9946-3846

Jeffrey Long
  University of California, Berkeley   https://orcid.org/0000-0002-5324-1321

Guangshan Zhu (✉ zhugs@nenu.edu.cn)
  Northeast Normal University

Article

Abstract

The use of coordination complexes as building units within covalent organic frameworks (COFs) has significant potential to diversify the structures and properties of this class of materials. Here, we present a synergistic coordination and reticular chemistry approach to the design of a series of crystalline scandium−covalent organic frameworks (Sc−COFs), featuring tunable levels of metal incorporation. Removal of scandium from the material with the highest metal content results in a metal-imprinted COF (MICOF) that exhibits high affinity and capacity for Sc^{3+} ions in acidic environments and in the presence of competing metal ions. In particular, the selectivity of this MICOF for Sc^{3+} over common impurity ions such as La^{3+} and Fe^{3+} surpasses that of all reported scandium adsorbents. Importantly, analogous materials can be prepared starting from earth-abundant transition metals, highlighting the versatility of this approach for the development of tailor-made metal−COFs and MICOFs for applications involving selective metal ion capture.

Background

Although considered one of the rare earth metals, scandium is not especially uncommon, with an abundance in the earth's crust similar to that of cobalt and lithium. However, mineral deposits rich in scandium are few, and scandium is largely sourced as a byproduct during the processing of iron, aluminum, lanthanide, and other ores[1−4]. Isolating scandium in useful quantities from these ores is extremely costly—concentrations are as low as 10^{-4} %[5], and the energy required for the extraction and processing of scandium is estimated at ~97 GJ/kg, at least two orders of magnitude greater than for the lanthanides[6,7]. As a result, scandium is very expensive and used to a limited degree in industry, despite its demonstrated value in applications such as lighting and high-performance alloys[8−10]. The development of new methods and materials for the selective and efficient extraction of scandium is therefore of great interest. Recent efforts have led to the discovery of ionic liquids[11,12], functionalized silicas[13], and gels[14] as candidates for scandium ion capture after leaching of metal ores.

Porous adsorbents including metal−organic frameworks[15] and organic frameworks[16] have been investigated as versatile and robust adsorbents for the capture of various metal ions. Among these materials, covalent organic frameworks (COFs)[17] have garnered particular interest, due to their low densities, high porosities, and chemical diversity. For example, two- and three-dimensional covalent organic frameworks featuring carboxylate[18,19], thioether[20,21], and EDTA functional groups[22] have been shown to capture mercury, cobalt, and the lanthanides with a high selectivity. In these materials, the capture functionality was installed post-synthetically at one of the organic building units or introduced as part of a primary building unit prior to framework synthesis. The same synthetic approaches have also been used in the design of so-called metal−covalent organic frameworks, which have attracted interest for applications such as catalysis, conductivity, and molecular separations, because they combine the electronic diversity accessible in metal−organic frameworks with the robustness of a structure buttressed purely by covalent bonds[24]. These hybrid materials have predominantly been generated *via* post-synthetic metalation, with the exception of two-dimensional variants prepared with metalated porphyrin or phthalocyanine monomers[23,24].

Inspired by this emergent chemistry and the complementary concept of molecular imprinting in porous materials[25−27], we envisioned a different paradigm for the preparation of metal−covalent organic frameworks that utilizes metal coordination complexes as *secondary* building units. Such an approach should enable a fine control over the extent of metal site incorporation, while also providing coordination sites selective for a given metal. Herein, we describe the design and synthesis of a new family of covalent organic frameworks, based on the parent material TpPa-1,[28] that feature varying quantities of Sc^{3+} coordination units (Fig. 1). The scandium ions can be liberated from these Sc−COFs to yield organic structures with "imprinted" metal coordination sites that, to our knowledge, have not previously been accessed in any other porous material. The imprinted framework with the highest density of coordination sites is highly selective for the uptake of Sc^{3+} over a number of other competing metal ions and is capable of extracting 98% of the scandium ions present in a nickel mineral sample with numerous competing metal ions at pH ~ 3. Notably, it is not necessary to use Sc^{3+} as the templating ion, and frameworks synthesized using secondary building units based on abundant divalent transition metal ions also yield metal-imprinted COFs (MICOFs) that are highly selective for scandium(III). The approach presented here affords a powerful means of designing diverse metal−covalent organic frameworks and imprinted covalent organic frameworks for selective metal ion capture.

Results And Discussion

Synthesis and characterization of Sc−COFs and metal-imprinted COFs. The robust, two-dimensional covalent organic framework TpPa-1 served as our model structure for the design of a porous organic framework featuring Sc^{3+} binding pockets[28]. The structure is built of repeating keto-enamine salicylideneaniline units and forms following the irreversible tautomerization of the enol-imine precursor synthesized from 1,3,5-triformylphloroglucinol and *p*-phenylenediamine (Fig. 1a). We identified 4-aminophenylacetate as a suitable ligand for the scandium-containing secondary building units, given

that Sc^{3+} readily forms trigonally-symmetric complexes with carboxylates[29], and further that energy minimization calculations indicated $Sc(C_8H_8NO_2)_3$ to be approximately the same size as the TpPa-1 repeat unit with pendant amine groups suitable for the formation of an extended TpPa-1-type structure (Fig. 1c). The $Sc(C_8H_8NO_2)_3$ complex was synthesized from the reaction of $ScCl_3 \cdot 6H_2O$ with 3 equiv. of 4-aminophenylacetic in a 4:1 (v:v) mixture of N,N-dimethylformamide and water (see Methods). The Fourier transform-infrared spectrum of $Sc(C_8H_8NO_2)_3$ features an absorption band at 1615 cm^{-1} that is redshifted from the −COOH stretch of the free ligand (1634 cm^{-1}) and was assigned to the asymmetric −COO stretch of a scandium-bound carboxylate (Supplementary Fig. 1)[29], while a new band at 520 cm^{-1} was assigned to a Sc−O vibration[29]. X-ray photoelectron spectra collected for $Sc(C_8H_8NO_2)_3$ and the known compound $Sc(O_2CC_{11}H_{23})_3$ ($O_2CC_{11}H_{23}^-$ = laurate)[29] both feature a single Sc_{2p} peak at ~400 eV, confirming the presence of scandium(III) in similar coordination environments (Supplementary Fig. 2).

Scandium-loaded covalent organic frameworks were prepared via the solvothermal reaction of $Sc(C_8H_8NO_2)_3$ with 1,3,5-triformylphloroglucinol and p-phenylenediamine in a mixture of mesitylene, dioxane, and aqueous acetic acid. Precise molar ratios were used to prepare the parent TpPa-1 structure and metal−covalent organic frameworks with scandium occupying 9% to 43% of the parent structure "nodes" (Fig. 1a; see Methods), referred to as Sc−COF-9 through Sc−COF-43. The occurrence of a Schiff base reaction in all cases and incorporation of Sc^{3+} was verified by infrared, X-ray photoelectron, and solid-state ^{13}C CP/MAS NMR spectroscopies, as well as by elemental analysis (Supplementary Figs. 2−4 and Table 1). Simulations performed in Materials Studio suggest that the substituted nodes in the Sc−COFs consist of one scandium ion coordinated by three 4-aminophenylacetate ligands, wherein the scandium center adopts a distorted octahedral geometry with an average Sc−O bond length of 2.18 Å[30,31] and a C−CH$_2$−C angle of 128.5° (Fig. 1c).

In the Sc−COF IR spectra, the characteristic −NH bands of p-phenylenediamine (3200−3500 cm^{-1}) are absent, while new bands associated with −C=C and −C−N vibrations are present at 1578 and 1255 cm^{-1} (Supplementary Fig. 3). All spectra additionally feature bands at 520 and 1616 cm^{-1}, assigned to a Sc−O vibration and the −COO stretch of a scandium-bound carboxylate, respectively. XPS characterization of Sc−COF-33 revealed a Sc_{2p} peak with an energy of ~400 eV identical to that of $Sc(C_8H_8NO_2)_3$ (Supplementary Fig. 2), confirming the presence of six-coordinate scandium(III) in the extended material. Finally, all peaks in the solid-state ^{13}C NMR spectrum of Sc−COF-33 could be assigned to the carbon atoms of the keto-enamine salicylideneaniline units or the scandium carboxylate ligands (Supplementary Fig. 4).

Powder X-ray diffraction data for Sc−COF-9 through Sc−COF-33 revealed that the structures crystallize in the $P6/m$ space group, retaining the symmetry of the parent TpPa-1 structure[28] (Supplementary Fig. 5a). Diffraction peaks centered at $2q$ = 4.7, 8.3, 12.6, and 27.0° are associated with the (100), (110), (210), and (001) crystal planes, respectively. The π-π stacking distance between the layers in the Sc−COFs was determined to be ~3.4 Å, based on the d spacing between the (001) planes[28]. Under identical

experimental conditions, the characteristic diffraction peak of the (100) plane at 4.7° was chosen to evaluate the relative crystallinity of the Sc−COFs. As the scandium complex content is increased from 0 to 33%, the relative intensity of the (100) peak remains unchanged, but there is a clear peak shift and reduction in intensity when the scandium incorporation reaches 43%. The apparent structural degradation may be attributed in part to limited stability of the molecular scandium complex under the solvothermal conditions (Supplementary Fig. 6). However, it is likely that the TpPa-1 structure is simply not stable to incorporation of scandium beyond ~33%, given that the inorganic building unit lacks the rigidity of the TpPa-1 repeating unit. Attempts to use tris(4-aminobenzoate) scandium(III) (without a methylene bridge), 4-aminophenylacetate, or larger 1,3,5-tris(4-aminobiphenyl) benzene as secondary building units in the construction of TpPa-1-type structures resulted in only amorphous materials, highlighting the importance of the size, tailored flexibility, and complex stability for framework synthesis (Supplementary Fig. 5).

Brunauer−Emmett−Teller (BET) surface areas of 660, 616, 570, 522, 485, and 431 m^2/g were determined for TpPa-1, and Sc−COF-9 through Sc−COF-33, respectively, from N_2 adsorption data collected at 77 K (Fig. 2a; Supplementary Figs. 7 and 8). Framework pore size distribution was determined using nonlocal density functional theory,[32] which revealed a peak at ~1.5 nm (Fig. 2b) in good agreement with the expected structure of TpPa-1. Scanning electron microscopy characterization of Sc−COF-33 revealed aggregated particles with sizes ranging from 1 to 5 μm (Supplementary Fig. 9), while transmission electron microscopy images reveal a highly ordered structure with pore size of 1.5 nm (Fig. 2e), consistent with the results of the pore size distribution analysis. The presence of scandium was confirmed by using aberration-corrected scanning transmission electron microscopy (STEM) (Fig. 2f). The high-angle annular dark field (HAADF)-STEM image of Sc−COF-33 features a multitude of bright dots corresponding to scandium ions that are well dispersed in the covalent matrix. The diameter of the dots is in the range of 2−3 Å, suggesting that each bright dot corresponds to one individual Sc^{3+} ion. An expanded view of a portion of this image further suggests that each dot is embedded in the ordered framework structure and that there is no scandium cluster formation.

The Sc−COFs were next treated with acid and base (see Methods) to release the scandium ions[33] and generate framework materials featuring open coordination sites, referred to as MICOF-9 through MICOF-33. The BET surface areas of these materials are slightly greater than the parent COFs, as expected upon removal of the scandium ions, while the narrow pore size distributions (Fig. 2c,d) suggest that they retain crystallinity and the TpPa-1 structure. Indeed, the powder X-ray diffraction pattern of MICOF-33 is indistinguishable from that of Sc−COF-33 (Supplementary Fig. 10), indicating that π−π interactions between adjacent layers are sufficient to stabilize the structure upon removal of the scandium ions. Elemental analysis of MICOF-33 revealed that less than 0.1% scandium remains in the structure after acid/base treatment (Supplementary Table 1), and thermogravimetric analysis revealed that the MICOFs are stable up to 250 °C (Supplementary Fig. 12).

Scandium uptake in MICOF-33. Scandium(III) adsorption data were collected at 298 K for MICOF-33 exposed to concentrations ranging from 2 to 500 ppm (pH ~ 5.5). The resulting adsorption isotherm (Fig.

3a) features an initial steep rise, indicating a strong affinity between the framework and Sc^{3+} ions, followed by a gradual plateau. At the highest examined Sc^{3+} concentration (500 ppm), the framework equilibrium capacity is 58.5 mg/g, corresponding to occupation of ~92% of the expected adsorption sites. The uptake data were fit with a Langmuir model (Fig. 3a, inset; see the Supplementary Information), yielding a saturation capacity of 58.9 mg/g that surpasses a number of reported scandium(III) adsorbents[14,34−36] (Supplementary Table 5). XPS characterization of MICOF-33 following scandium exposure revealed a Sc_{2p} peak with a binding energy identical to that of Sc−COF-33 and the scandium complex, confirming the successful uptake of Sc^{3+} at the vacant coordination sites (Supplementary Fig. 12). For the lowest initial Sc^{3+} concentration (2 ppm), 99.5% of the scandium was adsorbed after 48 h, corresponding to a large K_d of $2.01×10^6$ mL/g. MICOF-33 also exhibits rapid Sc^{3+} adsorption kinetics, as seen in Fig. 3b. Rapid metal ion uptake occurs in the first 5 min before beginning to plateau at ~10 min, and the framework achieves 82% of its saturation capacity (48.6 mg/g) after 180 min.

Depending on source, composition, and texture of a given mineral, there are many possible procedures that may be required for extracting pure metals, including ore pretreating, leaching, and solvent extraction[37]. Acidic leaching is a common process used to separate metal elements from mine tailings[37], and therefore it is highly desirable to realize an adsorbent capable of extracting scandium during the leaching stage. The uptake of Sc^{3+} in MICOF-33 and framework stability were accordingly examined under varying concentrations of HCl (Fig. 3c). The capacity Sc^{3+} decreases by less than 50% upon increasing the acid concentration by 100,000-fold, and even at the highest examined concentration of 10 M, the capacity remains moderate at 6.1 mg/g, exceeding the capacities of a number of scandium(III) adsorbents in the literature at higher pH values (Supplementary Table 5). Notably, MICOF-33 is also stable to repeated Sc^{3+} adsorption/desorption cycling at pH ~ 5.5 and exhibits a drop in capacity of only 0.7 mg/g (1.5%) after ten cycles (Fig. 3d).

Scandium ion selectivity. The selectivity of MICOF-33 for scandium(III) was examined by exposing a sample of the framework to an aqueous solution of HCl (pH ~ 3) containing 20 ppm of the Sc^{3+} ion and 10 ppm of a number of competing metal ions (Na^+, K^+, Mg^{2+}, Mn^{2+}, Fe^{2+}, Co^{2+}, Ni^{2+}, Zn^{2+}, Cd^{2+}, Al^{3+}, Cr^{3+}, Fe^{3+}, Y^{3+}, and La^{3+}; see the Supplementary Information). Importantly, the framework exhibits excellent selectivity for Sc^{3+} over all other examined metal ions (Fig. 4a), with selectivity coefficients (adsorbed mass ratios) ranging from $1.8×10^5$ (Sc^{3+}/K^+) to $1.1×10^2$ (Sc^{3+}/Fe^{2+}). The separation of iron(III) and scandium(III) is particularly challenging, given the similarity of their ionic radii and electronegativities[38], and MICOF-33 was also found to selectively capture Sc^{3+} over Fe^{3+} with a selectivity coefficient of 42. Of note, a control material with Tp, Pa, and 33% 4-aminophenylacetic acid as building units absorbed only 4.1 mg/g scandium(III) and exhibited far lower scandium selectivities ranging from 10.3 (Sc^{3+}/K^+) to 1.2 (Sc^{3+}/Al^{3+}) (Supplementary Fig. 14), highlighting critical role of ion imprinting to generate an adsorbent selective for Sc^{3+}. To our knowledge, the selectivity of MICOF-33 for Sc^{3+} over the common impurity ions La^{3+} (Fig. 4b and Supplementary Table 5) and Fe^{3+} (Supplementary Table 6) surpasses that of all Sc^{3+} adsorbents reported in the literature.

Significantly, it is not necessary to use scandium(III) as the template ion in the formation of scandium-selective MICOF-33. Indeed, it was possible to synthesize the framework instead using Ni^{2+}, Mg^{2+}, or Zn^{2+} complexes with 4-aminophenylacetate as secondary building units following the same synthetic protocol (see Supplementary Information). MICOF-33 samples prepared in this way exhibit similar scandium(III) uptake to the original MICOF-33 sample and retain high selectivity for scandium over Ni^{2+}, Mg^{2+}, or Zn^{2+}.

In order to elucidate the exceptional selectivity of MICOF-33 for Sc^{3+}, density functional theory (DFT) calculations were carried out to investigate the coordination environment of several different metal ions in a model complex featuring three 4-aminophenylacetate ligands. Calculations were implemented using Gaussian 16 code[42] with B3LYP/LANL2DZ+ empirical dispersion correction GD3[43]. The calculated Sc^{3+}–acetate bond energy of 1.39×10^3 kJ/mol is larger than that determined for various transition metal ions, Mg^{2+}, and Al^{3+} (0.54 to 1.21×10^3 kJ/mol; see Supplementary Fig. 19 and Supplementary Table 7), consistent with the selectivity of MICOF-33 for Sc^{3+} over these metal ions. The calculated bond energies for Y^{3+} and La^{3+} are competitive with that for Sc^{3+}, but uptake of these ions in MICOF-33 is far more sluggish: after 180 min, MICOF-33 achieves only 5.7% and 2.5% of its theoretical adsorption capacity for Y^{3+} and La^{3+}, respectively (Supplementary Table 8; c.f. 82% in the case of Sc^{3+}). Time-dependent uptake data for Y^{3+} and La^{3+} were fit using a pseudo-second order model (Supplementary Figs. 15 and 16) to yield k_2 values of 0.009 and 0.013 g/(mg•min), respectively, which are over an order of magnitude lower than that determined for Sc^{3+} (0.27 g/(mg•min)). It is likely that the larger ionic radii of these ions relative to Sc^{3+} impedes facile access to the coordination cavities in the framework.

Scandium extraction from minerals. A sample of nickel sulfide ore collected from Jilin, China was acidified (pH ~ 3) and treated with MICOF-33 to investigate the scandium(III) uptake properties of the framework from a real-world sample. After leaching, the initial metal ion solution was determined to contain Sc^{3+} (4.6 ppm), Al^{3+} (3.4 ppm), Fe^{3+} (1.2 ppm), Mg^{2+} (6.5 ppm), Ca^{2+} (222.1 ppm), Mn^{2+} (7.1 ppm), Co^{2+} (18.4 ppm), Ni^{2+} (3.5 ppm), Cu^{2+} (2.9 ppm), Zn^{2+} (1.7 ppm), Na^+ (2528.9 ppm), and K^+ (29.1 ppm) by ICP-MS. After 180 min, the MICOF-33 had adsorbed 98% of the Sc^{3+} present in the solution (corresponding to a capacity of 43.1 mg/g). Liberation of the captured scandium from the resulting sample using aqua regia yielded a filtrate with a scandium(III) purity greater than 96%, as determined by ICP-MS (96.84% Sc^{3+}, 2.55% Fe^{3+}, 0.40% Al^{3+}, 0.21% Mn^{2+}). Significantly, by carrying out five successive metal ion extraction and scrubbing operations (see Methods), it was possible to achieve a final Sc^{3+} purity as high as 99.90%, suitable for applications in lighting and high-powered lasers[44,45].

Conclusions

We have shown that the use of a specifically tailored Sc^{3+} coordination complex as a secondary building unit in the synthesis of the robust, two-dimensional framework TpPa-1[28] yields stable M−COFs that can be further treated to generate metal-imprinted frameworks selective for scandium ion capture. The material with the highest number of metal ion binding pockets exhibits excellent Sc^{3+} capacities,

selectivities, and cycling stability under acidic conditions, and it can be prepared from inexpensive, abundant transition metal ions, rendering it a promising candidate for practical utilization in scandium separation and purification. More broadly, we envision the synthetic approach presented here will serve as being a powerful and generalizable route toward the synthesis of a new class of hybrid metal–covalent organic frameworks and MICOFs with differing metal ions for diverse applications.

Methods

Preparation of Scandium Complex: $ScCl_3 \cdot 6H_2O$ (1 mM) and 4-aminophenylacetic acid (3 mM) were dissolved in a 2 mL *N,N*-dimethylformamide and water mixture (v/v 4:1) and stirred for 3 h at room temperature. Removal of the solvent under vacuum yielded $Sc(C_8H_8NO_2)_3$ as a colorless powder.

Preparation of Sc–COFs: Triformylphloroglucinol (25.2 mg, 0.120 mmol) was combined with *p*-phenylenediamine and $Sc(C_8H_8NO_2)_3$ in varying molar ratios to yield Sc–COF-9 (0.162 and 0.0120 mmol, respectively), Sc–COF-17 (0.144 and 0.024 mmol, respectively), Sc–COF-23 (0.126 and 0.0360 mmol, respectively), Sc–COF-29 (0.108 and 0.0480 mmol, respectively), and Sc–COF-33 (0.0900 and 0.0600 mmol, respectively). In each case, the reagents were combined together in a Pyrex tube with mesitylene (0.6 mL), dioxane (0.6 mL), and acetic acid (0.2 mL, 3 M). Each Pyrex tubes was sonicated to homogenize the mixture, flash frozen at 77 K, and degassed over three freeze–pump–thaw cycles. Finally, the Pyrex tubes were sealed and heated at 120 °C for 72 h. The tubes were then cooled to room temperature and the resulting solids were filtered, washed three times with *N,N*-dimethylacetamide and acetone, and then dried under vacuum at 100 °C to obtain the Sc–COFs.

Preparation of MICOFs: 1 M NaOH (10 mL) was added to each of the Sc–COF samples (10 mg), the mixtures were sonicated for 30 min, and the resulting solids were collected by filtration. The solids were then added to 1 M aqueous HCl (10 mL), the mixtures were sonicated for 30 min, and the solids were again isolated by filtration. The latter steps were repeated two times and the solids were collected by filtration and washed by distilled water (10 mL) and acetone (10 mL). The solids were finally dried under vacuum at 100 °C for 12 h, yielding the MICOF samples.

Purification of Scandium(III) from Nickel Ore: After initial metal ion uptake from the acidified ore sample, the metalated framework sample was treated (as described above) to yield MICOF-33 and a scandium(III)-rich filtrate. This filtrate was acidified to pH ~ 3 and the regenerated MICOF-33 sample was added to the solution and stirred for 180 min. Three additional adsorption/regeneration cycles were carried out in this manner to yield a scandium filtrate containing 99.90% pure Sc^{3+} ion, as determined by ICP-MS.

Declarations

Author contributions

Y.Y. and Y.Y. contributed equally. Y.Y. carried out the experiments and performed the data interpretation. X.G. and W.Z. performed the TEM and STEM characterizations. J.R.L. and K.R.M. helped design the experiments and wrote portions of the manuscript. S.Z. and R.F. conducted the theoretical calculations. Y.Y. and G.Z. developed the concept, supervised the experiments and drafted the manuscript.

Additional information

Supplementary information is available in the online version of the paper. Reprints and permissions information is available online at www.nature.com/reprints. Correspondence and requests for materials should be addressed to J.R.L. and G.Z.

Competing financial interests

The authors declare no competing financial interests.

References

1. Yasukawa, K. *et al.* A new and prospective resource for scandium: Evidence from the geochemistry of deep-sea sediment in the western North Pacific Ocean. *Ore Geol. Rev.***102**, 260–267 (2018).
2. Wang, W., Pranolo, Y. & Cheng, C. Y. Metallurgical processes for scandium recovery from various resources: a review. *Hydrometallurgy***108**, 100–108 (2011).
3. Wang, W. & Cheng, C. Y. Separation and purification of scandium by solvent extraction and related technologies: a review. *J. Chem. Technol. Biot.***86**, 1237–1246 (2011).
4. Makanyire, T., Sanchez-Segado, S. & Jha, A. Separation and recovery of critical metal ions using ionic liquids. *Adv. Manuf.***4**, 33–46 (2016).
5. Zhang, P., You, S., Zhang, L., Feng, S. & Hou, S. *Hydrometallurgy***47**, 47–56 (1997).
6. Wilson, A. M. *et al.* Solvent extraction: the coordination chemistry behind extractive metallurgy. *Chem. Soc. Rev.* **43**, 123–134 (2014).
7. Li, J., Chen, C., Zhang, R. & Wang, X. Reductive immobilization of Re (VII) by graphene modified nanoscale zero-valent iron particles using a plasma technique. *Sci. China: Chem.***59**, 150–158 (2016).
8. Das, S. *et al.* Extraction of scandium(III) from acidic solutions using organo-phosphoric acid reagents: A comparative study. *Sep. Purif. Technol.***202**, 248–258 (2018).

9. Ahmad, Z. The properties and application of scandium-reinforced aluminum. *JOM*, **55**, 35–39 (2003).

10. Das, S. *et al.* Extraction of scandium(III) from acidic solutions using organo-phosphoric acid reagents: A comparative study. *Sep. Purif. Technol.***202**, 248–258 (2018).

11. Makanyire, T., Sanchez-Segado, S. & Jha, A. Separation and recovery of critical metal ions using ionic liquids. *Adv. Manuf.***4**, 33–46 (2016).

12. Onghena, B. & Binnemans, K. Recovery of scandium(III) from aqueous solutions by solvent extraction with the functionalized ionic liquid betainium bis(trifluoromethylsulfonyl)imide. *Ind. Eng. Chem. Res.***54**, 1887–1898 (2015).

13. Tu, Z. *et al.* Silica gel modified with 1-(2-aminoethyl)-3-phenylurea for selective solid-phase extraction and preconcentration of Sc(III) from environmental samples. *Talanta***80**, 1205–1209 (2010).

14. Ramasamy, D. L., Puhakka, V., Doshi, B., Iftekhar, S. & Sillanpää, M. Fabrication of carbon nanotubes reinforced silica composites with improved rare earth elements adsorption performance. *Chem. Eng. J.***365**, 291–304 (2019).

15. Peng, Y. *et al.* A versatile MOF-based trap for heavy metal ion capture and dispersion. *Nat. Commun.***9**, 187 (2018).

16. Yuan, Y. & Zhu, G. Porous aromatic frameworks as a platform for multifunctional applications. *ACS Cent. Sci.* **5**, 409–418 (2019).

17. Diercks, C. S. & Yaghi, O. M. The atom, the molecule, and the covalent organic framework. *Science***355**, eaal1585 (2017).

18. Yue, J.-Y. *et al.* Metal ion-assisted carboxyl-containing covalent organic frameworks for the efficient removal of Congo red. *Dalton Trans.***48**, 17763–17769 (2019).

19. Lu, Q. *et al.* Postsynthetic functionalization of three-dimensional covalent organic frameworks for selective extraction of lanthanide ions. *Angew. Chem., Int. Ed.***57**, 6042–6048 (2018).

20. Huang, N., Zhai, L., Xu, H. & Jiang, D. Stable covalent organic frameworks for exceptional mercury removal from aqueous solutions. *J. Am. Chem. Soc.***139**, 2428–2434 (2017).

21. Sun, Q. *et al.* Postsynthetically modified covalent organic frameworks for efficient and effective mercury removal. *J. Am. Chem. Soc.***139**, 2786–2793 (2017).

22. Jiang, Y., Liu, C. & Huang, A. EDTA-functionalized covalent organic framework for the removal of heavy-metal ions. *ACS Appl. Mater. Interfaces* **11**, 32186–32191 (2019).

23. Dong, J., Han, X., Liu, Y., Li, H. & Cui, Y. Metal–covalent organic frameworks (MCOFs): a bridge between metal–organic frameworks and covalent organic frameworks. *Angew. Chem. Int. Ed.***59**, 2–14 (2020).

24. Feng, X., Ding, X. & Jiang, D. Covalent organic frameworks. *Chem. Soc. Rev.***41**, 6010–6022 (2012).

25. Chen, L., Wang, X., Lu, W., Wu, X. & Li, J. Molecular imprinting: perspectives and applications. *Chem. Soc. Rev.***45**, 2137–2211 (2016).

26. Yuan, Y., Yang, Y. & Zhu, G. Molecularly imprinted porous aromatic frameworks for molecular recognition. *ACS Cent. Sci.* DOI: 10.1021/acscentsci.0c00311 (2020).

27. Guo, Z. *et al.* Molecularly imprinted polymer/metal organic framework based chemical sensors. *Coatings***6**, 42 (2016).

28. Kandambeth, S. *et al.* Construction of crystalline 2D covalent organic frameworks with remarkable chemical (acid/base) stability via a combined reversible and irreversible route. *J. Am. Chem. Soc.***134**, 19524–19527 (2012).

29. Parashar, G. K. & Rai, A. K. Synthesis, molecular weights and infrared spectra of some scandium(III) higher carboxylates transition. *Met. Chem.***3**, 49–50 (1978).

30. St. Clair, M. A. & Santarsiero, B. D. Structure of a scandium–carboxylate complex: (η^5-$C_5Me_5)_2Sc(O_2C)C_6H_4CH_3$. *Acta Cryst.***C45**, 850–852 (1989).

31. Anderson, T. Neuman, M. & Melson, G. Coordination chemistry of scandium. VI.' Crystal and molecular structure of tris(tropolonato)scandium(III). Stereochemistry of some six-coordinate complexes. *Inorg. Chem.***13**, 158–163 (1974).

32. Ravikovitcha, P. I. Haller, G. L. & Neimark, A. V. Density functional theory model for calculating pore size distributions: pore structure of nanoporous catalysts. *Adv. Colloid Interfac.***76–77**, 203–226 (1998).

33. Jiang, J. Zhao, Y. & Yaghi, O. M. Covalent chemistry beyond molecules. *J. Am. Chem. Soc.* **138**, 3255–3265 (2016).

34. Zhang, N. Huang, C. & Hu B. ICP-AES Determination of trace rare earth elements in environmental and food samples by on-line separation and preconcentration with acetylacetone-modified silica gel using microcolumn. *Anal. Sci.***23**, 997–1002 (2007).

35. Iftekhar, S. Srivastava, V. & Sillanpää, M. Enrichment of lanthanides in aqueous system by cellulose based silica nanocomposite. *Chem. Eng. J.***320**, 151–159 (2017).

36. Ramasamy, D. Puhakka, V. Repo, E. Khan, S. & Sillanpää, M. Coordination and silica surface chemistry of lanthanides (III), scandium (III) and yttrium (III) sorption on 1-(2-pyridylazo)-2-napththol (PAN) and acetylacetone (acac) immobilized gels. *Chem. Eng. J.***324**, 104–112 (2017).

37. Wang, W., Pranolo, Y. & Cheng, C. Y. Metallurgical processes for scandium recovery from various resources: A review. *Hydrometallurgy* **108**, 100–108 (2011).

38. Shannon R. D. Revised effective ionic radii and systematic studies of interatomic distances in halides and chalcogenides. *Acta Cryst.* **A32**, 751–767 (1976).

39. Ramasamy, D. Puhakka, V. Repo, E. Hammouda, S & Sillanpää, M. Two-stage selective recovery process of scandium from the group of rare earth elements in aqueous systems using activated carbon and silica composites: Dual applications by tailoring the ligand grafting approach. *Chem. Eng. J.***341**, 351–360 (2018).

40. Lou, Z. *et al.* Acrylic Acid-Functionalized Metal–Organic Frameworks for Sc(III) selective adsorption. *ACS Appl. Mater. Interfaces*. **11**, 11772-11781 (2019).

41. Giret, S. *et al*. Selective separation and preconcentration of scandium with mesoporous silica. *ACS Appl. Mater. Interfaces.* **10**, 448–457 (2018).

42. Frisch, M.J. *et al*. Gaussian 16 *Rev. C.***01**, Wallingford, CT (2016).

43. Wei, D. *et al*. Adsorption Properties of Hydrated Cr^{3+} Ions on Schiff-base Covalent Organic Frameworks: A DFT Study. *Chemistry − An Asian Journal***15**, 1140-1146 (2020).

44. Spedding, F. H. & Croat, J. J. Magnetic properties of high purity scandium and the effect of impurities on these properties. *J. Chem. Phys.***58**, 5514−5526 (1973).

45. Bunzli, J.-C. G. & Choppin, G. R. Lanthanide probes in life, Chemical and Earth Sciences (Elsevier, Amsterdam, 1989).
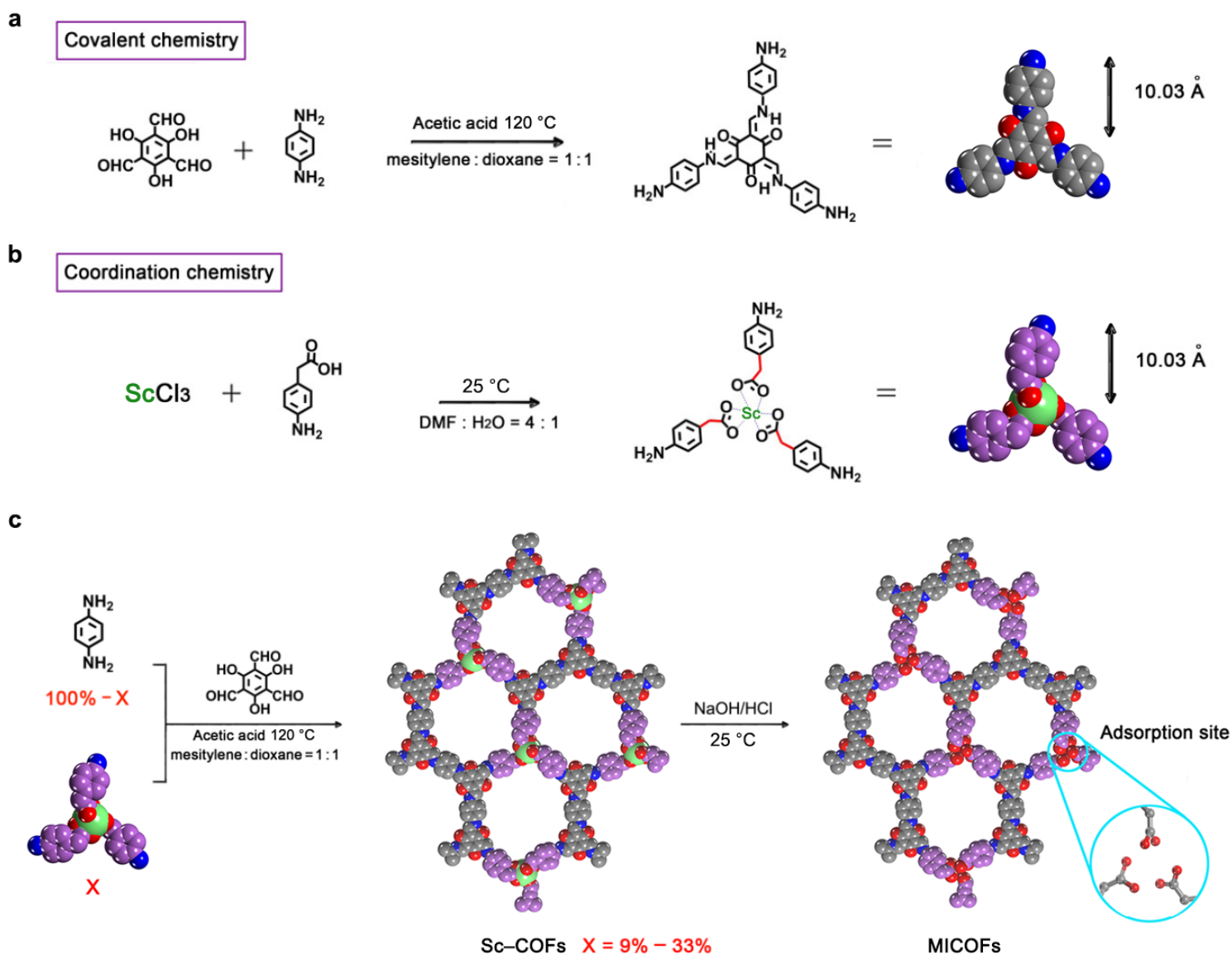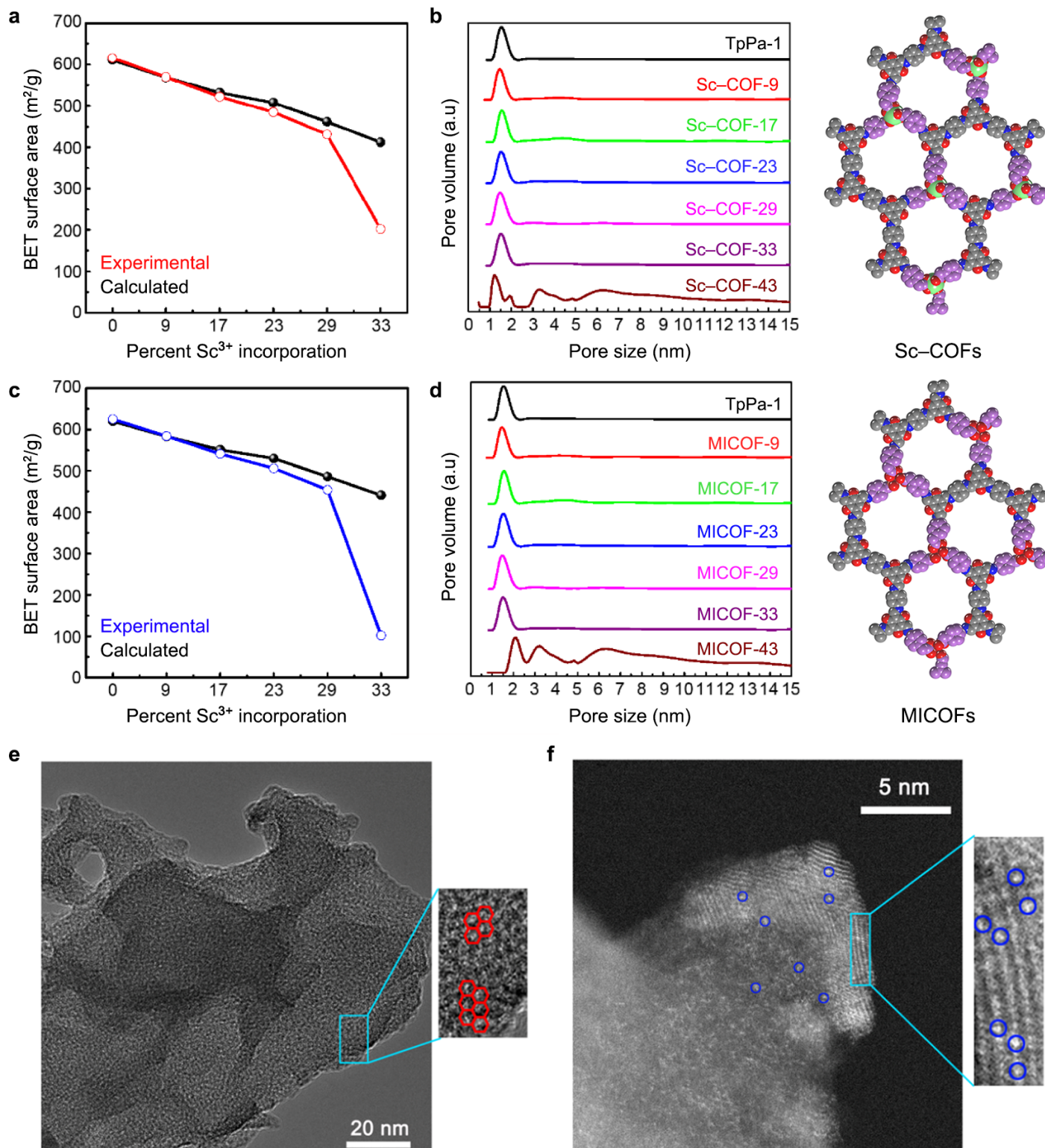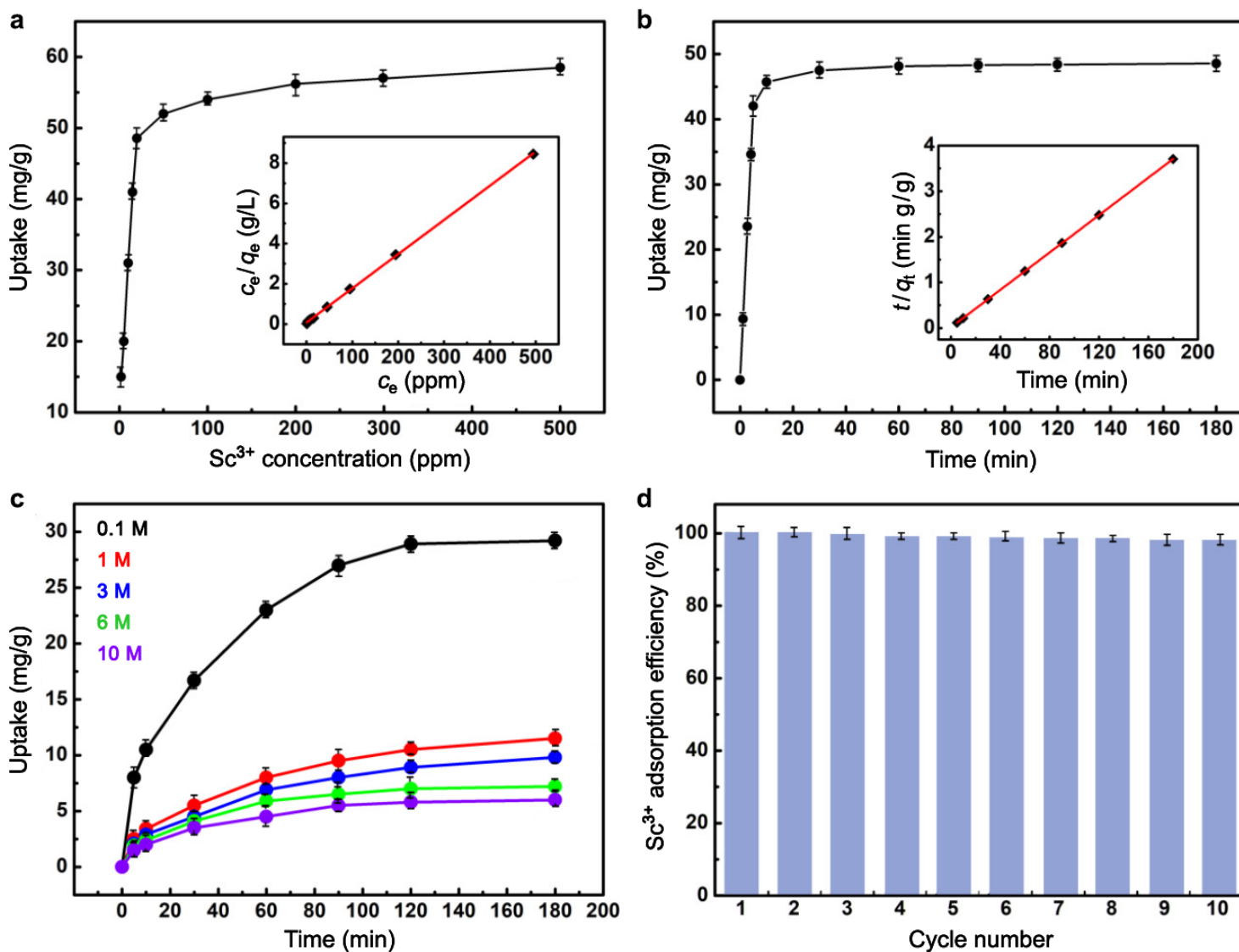
Figures

Figure 1

Strategy for Sc−COFs and metal−imprinted COFs. a, The parent COF structure chosen for this study, TpPa-1, is constructed from repeating keto-enamine salicylideneaniline units. b, In order to mimic the size, functionality, and geometry of the TpPa-1 building units for the design of a hybrid scandium COF, 4-aminophenylacetate was chosen as a ligand for the design of trigonal scandium complex secondary building units. c, Sc−COFs were prepared with varying degrees (9, 17, 23, 29, 33%) of scandium ion incorporation. The Sc3+ ions can subsequently be removed to generate metal-imprinted COFs, or MICOFs, with open coordination sites.

Figure 2

Characterization of Sc−COF-33. Experimental and theoretical BET surface areas and pore size distributions for a−b, Sc−COFs and c−d, MICOFs. The theoretical surface areas were determined starting from the TpPa-1 BET surface area and calculating the change in mass and specific surface area upon replacing the COF structural unit with the varying quantities of the scandium(III) complex. e, TEM image of Sc−COF-33 where the 1.5 nm pores are highlighted with red hexagons. f, HAADF-STEM image of Sc−COF-33 where scandium ions can be visualized as white dots; select scandium positions are highlighted with dark blue circles.

Figure 3

Scandium(III) uptake in MICOF-33. a, A scandium(III) adsorption isotherm collected for MICOF-33 at 298 K upon exposure to solutions of scandium(III) chloride hexahydrate dissolved in aqueous HCl (pH ~ 5.5) with initial concentrations as indicated. Inset: Equilibrium adsorption data and fit using a Langmuir model ($R2 = 0.9998$; see the Supplementary Information for details), yielding a saturation capacity of 58.9 mg/g. b, Scandium(III) uptake as a function of time in MICOF-33 after exposure to a 20 ppm solution

of aqueous scandium(III) chloride hexahydrate (pH ~ 5.5). Inset: Fit of the time-dependent uptake data to a pseudo-second order model (k2 = 0.27 g/(mg•min), R2 = 0.9999, see the Supplementary Information for details). c, Time-dependent scandium(III) uptake in MICOF-33 as a function of HCl concentration. d, Cycling data for scandium(III) uptake in MICOF-33 from a 20 ppm aqueous solution (pH ~ 5.5). Over the course of ten cycles, the capacity decreases by only 1.5%.
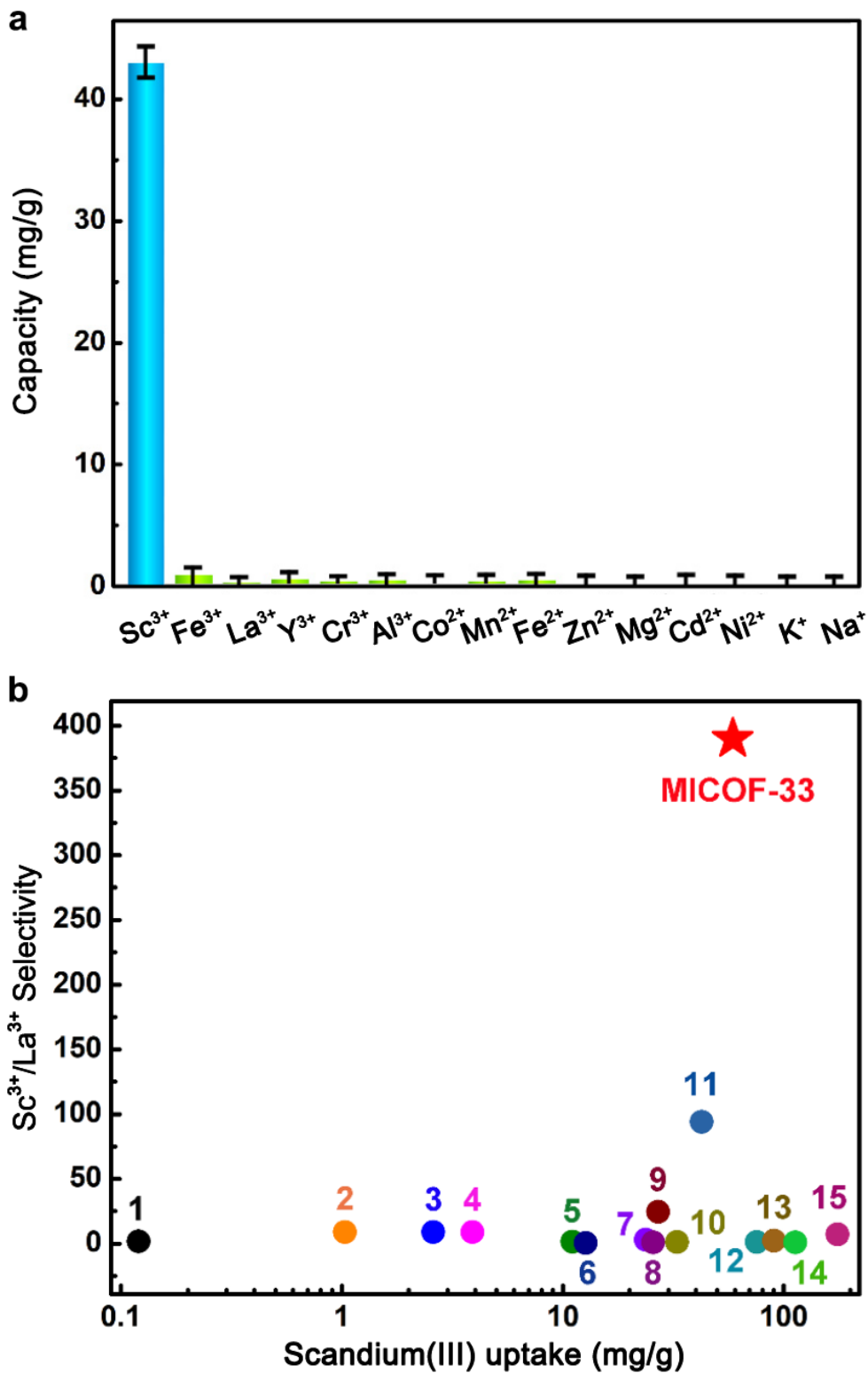

Figure 4

Scandium(III) uptake selectivity. a, Comparison of the equilibrium uptake of Sc3+ and various other metal ions in MICOF-33. b, Sc3+/La3+ selectivity of MICOF-33 and reported adsorbents for scandium(III) capture. See Supplementary Table 5 for a full list of adsorbents, references, and associated adsorption metrics.

Supplementary Files

This is a list of supplementary files associated with this preprint. Click to download.

- SupplementaryInformation.docx
- SupplementaryInformation.docx